

METHOD OF MEASUREMENT OF ELECTRON ENERGIES AND OTHER DATA FROM SPECTROGRAMS OF V.L.F. EMISSIONS

By R. L. DOWDEN*

[*Manuscript received August 8, 1962*]

Summary

It has been shown that the detailed frequency-time shape of discrete very low frequency emissions from the exosphere can be closely fitted on the electron-cyclotron theory by suitably choosing the electron parameters. Additional support for the theory has since been obtained in the verification of its prediction. It is shown here that the fitting process can be reversed so that these parameters can be deduced from the observed spectrograms. These are: the energy and helical pitch of the emitting electrons, the field line which guides them, the instant of their passing through the equatorial plane, and the electron density of the medium. Nomograms are given allowing calculation of these with occasional use of a slide rule and simple arithmetic.

I. INTRODUCTION

In a recent paper (Dowden 1962*a*) it was pointed out that the cyclotron radiation from an electron spiraling along a geomagnetic field line *away* from the observer will be Doppler shifted to a frequency appreciably less than the frequency of gyration of the electron. An electron (or rather a small bunch of electrons) travelling from the observer's hemisphere to the opposite hemisphere will radiate at a decreasing frequency until it crosses the equatorial plane, and thence at an increasing frequency. Consideration of electron travel times and wave-group propagation times gives the frequency-time (spectrogram) shape of a "hook" for such a hemisphere to hemisphere traverse.

Other types of discrete emissions ("chorus", "risers", "pseudo noses", "falling tones", etc.) are produced by incomplete traverses. In particular the theory predicted a repetitive type emission when the electron bunch survives several hemisphere to hemisphere traverses or "bounces" between magnetic mirror points. Occurrences of this type have since been shown (Dowden 1962*b*) and the observed bounce periods (hook repetition period) agreed well with those calculated from electron parameters deduced (by the method to be discussed here) from the frequency-time shape of the individual hooks.

The parameters which affect the frequency-time shape, scale, and position of the complete transverse emission ("hook") as observed on the Earth are: the energy E and helical pitch ψ of the emitting electrons, the terminal geomagnetic latitude λ of the field line which guides them, the instant ($\frac{1}{2}t_0$) of their passing through the top of this field line, and the "scale frequency" a of the electron density of the medium. If these are suitably chosen a theoretical frequency-time trace can be calculated to give an effectively exact fit to any

* Ionospheric Prediction Service, University of Tasmania, Hobart.

observed hook. This has been demonstrated with a relatively complex hook (Dowden 1962*b*). This and the later verification of the prediction mentioned above effectively establish the theory. In addition the observed trace contains the effects of these parameters so that it may be possible to deduce these parameters from the observed trace.

It will be shown here that the scaling of only two frequencies (f_n and f_0) and two times (T^+ and T^-) is sufficient for complete and unambiguous evaluation of the parameters cited above.

II. ENERGY

The general expression for the Doppler-shifted cyclotron frequency from an electron spiraling along a field line is (Eidman 1958)

$$f = h[\gamma(1 \pm \beta_d \cos \theta)]^{-1}, \quad (1)$$

where h is the local gyro frequency, γ is the relativistic correction $(1 - \beta^2)^{-1/2}$, n is the refractive index of the medium at the frequency f , β_d is the longitudinal component of velocity in units of the velocity of light, and θ is the angle between the field and the direction of emission.

The minus sign in (1) refers to forward Doppler shift and so need not be considered here. The angle θ in (1) also appears in the general Appleton-Hartree expression for the refractive index. For the terrestrial case of backward Doppler-shifted emission the general expression for f obtained by substituting this refractive index $n(\theta)$ into (1) is found (Ellis 1962) to be almost independent of θ . If it were otherwise we would not expect such narrow-band V.L.F. emissions as are observed. Consequently we consider only the case $\theta = 0$.

The whistler mode refractive index is given by

$$n^2 = 1 + p^2[f(h - f)]^{-1}, \quad (2)$$

where p is the plasma frequency of the medium. This latter can be expressed in the form

$$p^2 = ah,$$

where a is the "scale frequency" (Dowden 1962*c*). For a gyro frequency model (electron density everywhere proportional to magnetic field or gyro frequency), as suggested by whistler data (Smith 1960), a is constant.

From (1) and (2), making the appropriate substitutions discussed above, and for $n^2 \gg 1$, we have

$$(h - f)(h/\gamma - f)^2 = a\beta_d^2 hf. \quad (3)$$

This more general expression reduces to that obtained previously (Dowden 1962*a*) for $\gamma = 1$. If ψ is the helical pitch angle we have

$$\beta_d = \beta \cos \psi.$$

The helical pitch at any point is determined by its value at any other point by the principle of invariance of magnetic moment. Thus, specifying quantities in the equatorial plane by subscript zero, we have

$$\beta_d^2 = \beta^2 [1 - \gamma \sin^2 \psi_0], \quad (4)$$

where η is the ratio of the magnetic field or gyro frequency at the point in question to that at the equatorial plane. For a dipole field

$$\eta = (1 + 3 \sin^2 l)^{1/2} \sec^6 l,$$

where l is the latitude coordinate angle.

At the equatorial plane ($l=0$) we have from (3) and (4)

$$(h_0 - f_0)(h_0/\gamma - f_0)^2 = a\beta^2 \cos^2 \psi_0 h_0 f_0. \quad (5)$$

Making the substitution $x = h_0/f_0$ and $\beta^2 = (\gamma^2 - 1)/\gamma^2$ we get

$$\frac{\gamma^2 - 1}{\gamma^2} = \frac{f_0}{a \cos^2 \psi_0} \frac{[x - 1]^3}{x} \left[\frac{x/\gamma - 1}{x - 1} \right]^2. \quad (6)$$

The kinetic energy of an electron is given by

$$E = 500(\gamma - 1) \text{ keV}. \quad (7)$$

As we will find later, nearly all emissions are produced by electrons of energies for which relativistic effects are very small ($\gamma \simeq 1$).

For these we can write

$$E' = 250\beta^2 = (250f_0/a \cos^2 \psi_0)(x - 1)^3/x \text{ keV}. \quad (8)$$

From (6), (7), and (8) we find

$$E' = E(1 + E \times 10^{-3})[(x - 1)/(x - \gamma)]^2. \quad (9)$$

From (8) we would generally expect high energies to be associated with large values of x , in which case the term containing x is close to unity and (9) is in a convenient form for applying relativistic corrections to a nomogram energy scale. This is shown in Figure 4.

Of the quantities in (8) required for evaluation of the electron energy only f_0 is measurable in an obvious manner from spectrograms of complete emissions ("hooks"). This is the minimum or cusp frequency of the hook (for $\gamma \simeq 1$) as shown previously (Dowden 1962*a*). We now consider methods of deducing the other parameters.

III. LATITUDE λ AND PARAMETER x

Suppose we assume that the energy lost (radiated) by the bunch during one hemisphere to hemisphere traverse is negligible. Then the observed emission frequencies will be symmetric with respect to the geomagnetic equatorial plane. That is, the frequency produced by the bunch at latitude angle l in the northern hemisphere will be the same as that produced when this bunch is at the same latitude angle in the southern hemisphere.

Consider the hook in Figure 1 as observed in the northern hemisphere. We require the times T_1 and T_2 for some frequency f . These times, which define the shape of the hook, are made up of group propagation times (t_g) of waves of frequency f and f_0 and electron bunch travel times (t_e). We can specify a point on a given line of force by the gyro frequency at that point. Suppose that at the two points (one in each hemisphere) where the frequency f is produced, the

gyro frequency is h . The equatorial plane is then denoted by h_0 and the Earth's surface by h_λ . Propagation times along the surface of the Earth to the observer do not involve dispersion and so do not change the shape of the hook.

Consequently the time T_1 is the time taken for the electron bunch to travel from the point h_N in the northern hemisphere where frequency f is produced to the equatorial plane (h_0) plus the difference between the propagation times for

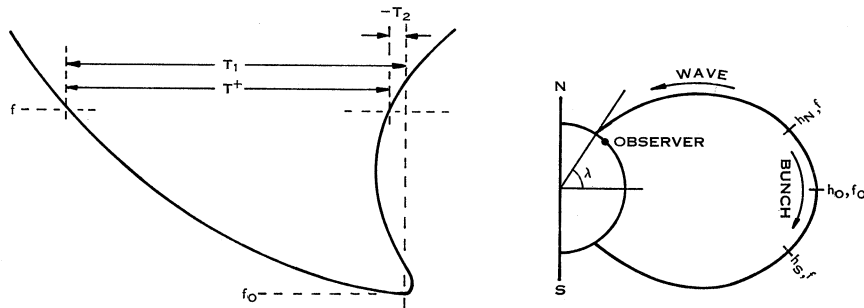


Fig. 1.—A tracing of a frequency-time spectrogram of a hook and the path of the electron bunch which generated it.

frequency f_0 to travel from the equatorial plane (h_0) to the Earth's surface ($h_{\lambda N}$) in the northern hemisphere and that for frequency f to travel from point h_N to $h_{\lambda N}$. Putting this in symbolic form,

$$T_1 = t_e(h_N \rightarrow h_0) + t_g(f_0, h_0 \rightarrow h_{\lambda N}) - t_g(f, h_N \rightarrow h_{\lambda N}).$$

In a similar way we find

$$\begin{aligned} T_2 &= t_e(h_0 \rightarrow h_S) + t_g(f, h_S \rightarrow h_{\lambda N}) - t_g(f_0, h_0 \rightarrow h_{\lambda N}) \\ &= t_e(h_0 \rightarrow h_S) + t_g(f, h_S \rightarrow h_0) + t_g(f, h_0 \rightarrow h_N) \\ &\quad + t_g(f, h_N \rightarrow h_{\lambda N}) - t_g(f_0, h_0 \rightarrow h_{\lambda N}). \end{aligned}$$

We can drop the N, S subscripts if we always refer to the shortest distance. Taking the sum and difference times T^+ and T^- we find :

$$T^+ = T_1 + T_2 = 2t_e(h_0 \rightarrow h) + 2t_g(f, h_0 \rightarrow h), \quad (10)$$

$$T^- = T_1 - T_2 = 2t_g(f_0, h_0 \rightarrow h_\lambda) - 2t_g(f, h_0 \rightarrow h_\lambda). \quad (11)$$

We will discuss (10) later. Consider now the difference time T^- given by (11). This contains only wave propagation times. Furthermore, if we consider T^- as a function of frequency f , then (11) is the general (nose) equation of a "short" whistler centred on the time ($T^- = 0$) for which $f = f_0$. The frequency for which T^- is maximum is then the nose frequency f_n of the equivalent nose whistler. Measurement of f_n defines the line of force in which the hook is produced and along which the electron bunch is guided. A function given by Smith (1960) enables h_0 and λ to be found from f_n .

A simple but accurate way of measuring f_n is shown in Figure 2. The frequency-time shape of the hook is traced on transparent paper. This tracing is turned over onto the original hook so that the frequency scales still correspond.

By moving the tracing in the time direction a position will be found where the descending part of the traced hook just touches the ascending part of the original hook and vice versa. The frequency at which this occurs is then the "true" nose frequency f_n . Note that this is always higher than the pseudo nose which sometimes appears on the ascending part of the hook (Fig. 2).

The nose frequency difference time (T_n^-) can be found at the same time, as shown in Figure 2. We have shown that $T^-(f)$ defines the exact shape of a whistler and so should provide electron density information. Smith and Carpenter (1961) have shown that if the time delays (t) and frequencies (f) of

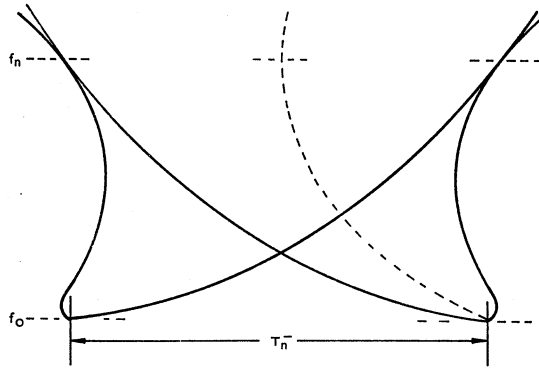


Fig. 2.—Method of scaling the nose frequency and difference time at this frequency. The midpoint locus (broken curve) has the shape of a nose whistler.

whistlers are normalized to nose values (t_n and f_n) then the resulting curves of t/t_n versus f/f_n all closely fit a single "universal whistler dispersion function" which they have calculated. Our T_n^- is then

$$T_n^- = t_0 - t_n,$$

that is,

$$T_n^-/t_n = S(f_0/f_n) - 1, \quad (12)$$

where t_0 is the short whistler time delay at frequency f_0 , and S is the Smith-Carpenter dispersion function. The double-sided scale shown in Figure 3, which has been constructed from this function, allows calculation of t_n . Note that we can also find the time $\frac{1}{2}t_0$, which is the time between the instant the electron bunch passes through the equatorial plane (where frequency f_0 is emitted) to the instant of reception on the Earth of the cusp or minimum frequency of the hook.

It is interesting to consider here an alternative method of finding f_n and T_n^- which illustrates some of the points made above. The mid point of a line drawn from some frequency f on one branch of the hook to the same frequency on the other branch is given by

$$T_1 - \frac{1}{2}T^+ = \frac{1}{2}T^-.$$

Thus the locus of the mid point is the whistler which would be observed if a wide-band impulse occurred at the instant the electron bunch passed through the equatorial plane. This "half whistler" is shown in Figure 2. This alternative method is useful for finding f_n when the hook does not extend to this frequency by using the Smith-Carpenter techniques, particularly if the scale frequency (discussed below) is known from other data.

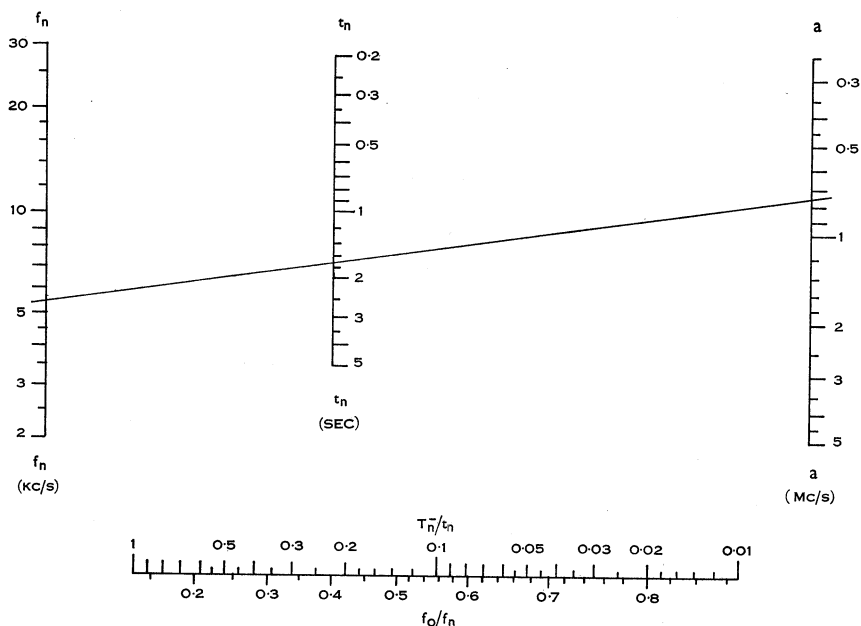


Fig. 3.—Nomogram for calculation of scale frequency a .

Having found t_n , f_n by the methods outlined above, or more accurately perhaps by the use of real nose whistlers we can now find the scale frequency a . This is given by (Dowden 1962c)

$$a = N(f_n) f_n^{5/3} t_n^2,$$

where N is a slowly varying function. A nomogram for solving this equation is given in Figure 3. The function N has been built into the f_n scale.

IV. HELICAL PITCH

The sum time T^+ is the time width of the hook at any given frequency, as shown in Figure 1. From equation (10) we see it contains both wave propagation times and electron bunch travel times. Thus T^+ will be dependent on ψ_0 so that it should be possible to use T^+ as a measure of ψ_0 .

Suppose we measure T^+ at frequency $f = 2f_0$. For a dipole field we have

$$2t_e = 2 \int_0^l \frac{R_0 \cos \psi_0 \cdot \eta \cos^7 l dl}{\beta c [1 - \eta \sin^2 \psi_0]^{1/2}}.$$

In (13) and (14) the integration limits l and η refer to values at the level for which $f=2f_0$ (and $h=\eta h_0$). At this level we have from (3) and (4) for the non-relativistic case

$$[\eta h_0 - 2f_0]^3 = a\beta^2 \cdot 2f_0 \cdot \eta h_0 [1 - \eta \sin^2 \psi_0].$$

At the equatorial plane ($f=f_0$) we have

$$[h_0 - f_0]^3 = a\beta^2 f_0 h_0 \cos^2 \psi_0.$$

Dividing and making the x substitution

$$[(\eta x - 2)/(x - 1)]^3 = 2\eta [1 - \eta \sin^2 \psi_0] / \cos^2 \psi_0. \quad (15)$$

We can now find η from (15) and l from η and substitute these into (13) and (14). Then from (10) we have

$$T^+ = a^{1/2} f_0^{-5/6} F(x, \psi_0), \quad (16)$$

where F is a function of x and ψ_0 but not of η . For a given value of F , which can be calculated from observed values of T^+ , a , and f_0 , then ψ_0 is a function of x only. This is shown by the family of curves of constant F in Figure 4. In this nomogram (Fig. 4) a point on the x scale is found from f_0 and f_n and a point in the F scale from f_0 and T^+ (for $a=1$ Mc/s). With the help of the nose-shaped curve the appropriate F curve is selected. This curve will intercept the previously found x value at the ψ_0 value given by the top scale.

The highest frequency observed on the rising part of a hook is about $0.5-0.6h_0$. This effect is well known in whistler studies (Smith 1960) and is caused by high attenuation in the vicinity of the gyro frequency. Thus measurement of T^+ at $f=2f_0$ is not possible for hooks of $x < 3$ or 4. Also it will be noted from Figure 4 that the F curves become nearly horizontal for low values of x . For such hooks we use an alternative method based on T^+ measurement at $f=f_n$ or in general at $f=gh_0$.

Equation (15) becomes

$$[(\eta - g)/(x - 1)]^3 = \eta g [1 - \eta \sin^2 \psi_0] / x^2 \cos^2 \psi_0.$$

Rearranging,

$$x^2/[x - 1]^3 = \eta g [1 - \eta \sin^2 \psi_0] / [\eta - g]^3 \cos^2 \psi_0 = X_1. \quad (17)$$

From (8) and (17) we find

$$\beta^2 = \frac{h_0}{a} \cdot \frac{[\eta - g]^3}{\eta g [1 - \eta \sin^2 \psi_0]}.$$

Substituting this into the integral for $2t_e$ we find

$$2t_e = 8 \cdot 4 a^{1/2} h_0^{-5/6} \cdot \frac{\eta^{1/2}}{[\eta - g]^{3/2}} \cdot [1 - \eta \sin^2 \psi_0]^{1/2} \int_0^l \frac{\eta \cos^7 l dl}{[1 - \eta \sin^2 \psi_0]^{1/2}}.$$

Note that this does not contain x . Also to the extent that

$$\frac{[1 - \eta \sin^2 \psi_0]^{1/2}}{l} \int_0^l \frac{\eta \cos^7 l dl}{[1 - \eta \sin^2 \psi_0]^{1/2}} = 1, \quad (18)$$

and using the approximation for small values of l ,

$$l \approx \frac{\sqrt{2}}{3} [\eta - 1]^{1/2}.$$

we have

$$2t_e = 3 \cdot 96 a^{1/2} h_0^{-5/6} \eta^{1/2} \cdot [\eta - 1]^{1/2} / [\eta - g]^{3/2}. \quad (19)$$

Using the same quasi-constant model of electron density and referring all frequencies to h_0 , we find

$$2t_g = \frac{6 \cdot 06}{g^{1/2} [1 - g]} a^{1/2} h_0^{-5/6} \frac{\eta - 1}{\eta^{1/2}} [\eta - g]^{-1/2}. \quad (20)$$

So that from (10) we have

$$T^+(g) = a^{1/2} h_0^{-5/6} G(g, \eta), \quad (21)$$

where G is given by (19) and (20).

The error introduced into t_e by assuming the validity of (18) is very small at low frequencies (near f_0) where $t_e > t_g$. It becomes larger at the higher frequencies, but there $t_g > t_e$ so that the resulting error in T^+ is never appreciable. It may seem surprising then that G , which does not contain ψ_0 explicitly, can be used to find ψ_0 . However, we can obtain η by inverting G and then, solving (17) for ψ_0 , we have

$$\sec^2 \psi_0 = \frac{1}{\eta - 1} \left[\eta - \frac{X_1(\eta - g)^3}{\eta g} \right]. \quad (22)$$

V. USE OF NOMOGRAMS

We have obtained expressions for the electron parameters E , ψ_0 , λ , t_0 , and a in terms of the quantities f_0 , f_n , T_n^- , and T^+ which can be scaled from spectrograms of hooks as explained above. We now discuss techniques of evaluation of these parameters using the nomograms of Figures 3, 4, and 5.

The scale frequency a is found from the nomogram of Figure 3. The f_n , t_n data may be taken from (i) the hook to which one is to apply the scale frequency value for calculation of other parameters, (ii) a nearby hook, or (iii) a nose or "near-nose" whistler. In the first two cases t_n is deduced from f_0 , f_n , and T_n by use of the double-sided scale in Figure 3. It will be seen from this scale that for reasonable accuracy we require a hook for which $f_n \gtrsim 2f_0$. In general, whistler measurements will be more accurate. However, in both cases (ii) and (iii) we may be measuring scale frequency in a different field line (if f_n is different). This could introduce an error of 40% (Smith 1960).

For evaluation of the other parameters T^+ is measured at $f = 2f_0$ and the nomogram of Figure 4 is used, provided $f_n \gtrsim 2f_0$. Otherwise T^+ is measured at $f = f_n$ or $f = \frac{3}{4}f_n$ and Figure 5 is used. In both cases the terminating geomagnetic latitude of the field line is immediately obtained from the f_n - λ scale.

Consider the first case (Fig. 4). The f_0 scale is graduated and scaled logarithmically in f_0 . The f_n - λ scale is scaled (but not graduated) logarithmically in h_0 . A straight line through appropriate values of f_0 and f_n gives the position of x on the x reference line. This scale is not graduated as the actual value is

not required. Similarly the position of F on the F reference line can be found from f_0 and T^+/\sqrt{a} . The curve labelled X_2 is the function

$$X_2 = (x-1)^3/x.$$

The position of X_2 on the X_2 reference line, corresponding to x found above, is obtained by drawing a horizontal line through the x point and a vertical line through the X_2 point such that these intersect on the X_2 curve. A horizontal line drawn through the F point will intersect the nose-shape curve at a point which lies on the appropriate constant F curve of the family. This curve will intersect the horizontal line through x at the value of ψ_0 given by (vertical line) the ψ_0-l_m scale at the top of Figure 4. This scale is graduated in degrees for

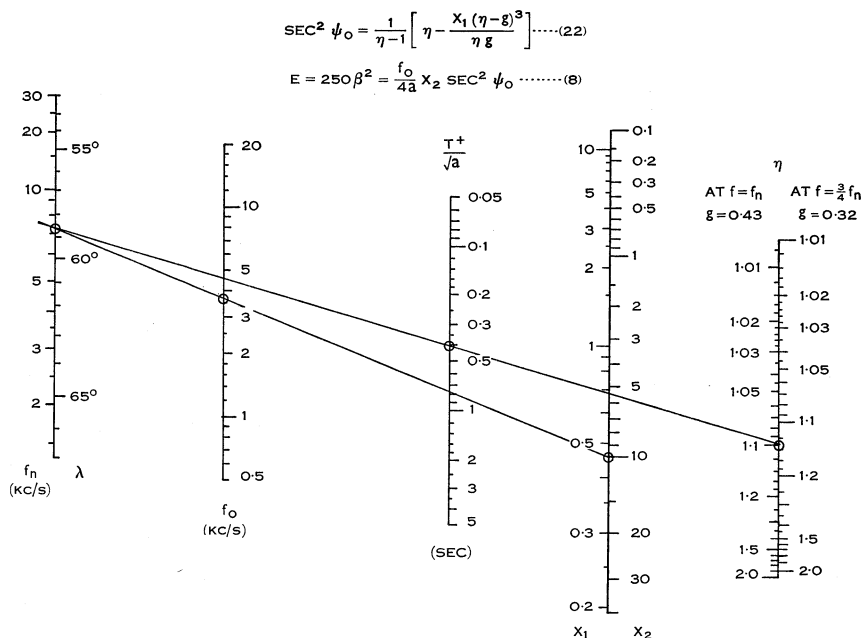


Fig. 5.—Nomogram for calculation of η , X_1 , and X_2 for T^+ measured at the nose frequency or three-quarters of this frequency. Energy and helical pitch are then obtained from the expressions (8) and (22). This method entails some simple arithmetic and slide rule calculations.

ψ_0 and l_m (latitude angle of mirror point) but scaled logarithmically in $\sec^2 \psi_0$. The energy (E) and β are then found from f_0/a , the position X_2 and $\sec^2 \psi_0$ nomographically. This part of the nomogram expresses equation (8). The E - β scale is scaled logarithmically in E' but graduated according to the relativistic correction given in equation (9).

This procedure is illustrated by the example shown in Figure 4. Only certain combinations of scales bear nomographic relationships so meaningful intercepts are marked with small circles. It is, of course, unnecessary to draw any of these lines or curves. All scales and reference lines are parallel or perpendicular so that set squares can be used for the graphical parts. It should

be noted that the scale frequency must be used in units of Mc/s as obtained in Figure 3.

If $f_n < 2f_0$, measurement at $f = 2f_0$ may be impossible. In this case the nomogram of Figure 5 is used. The value of η is found from the f_n and T^+/\sqrt{a} scales. The η scale is logarithmically scaled in the function G of equation (21) but graduated in η for two values of g . As will be seen later, the terminal latitudes (λ) of the field lines in which hooks are generated appear to be confined to a narrow range about 60° . For this range these two values correspond to $f = f_n$ and $f = \frac{3}{4}f_n$. The time T^+ can be measured at either of these frequencies provided the corresponding side of the η scale is used. The X_1 - X_2 scales are scaled logarithmically in x and so these values are obtained from the f_n and f_0 scales as shown in Figure 5. Then E , β , and ψ_0 must be calculated from equations (22) and (8). Since this case ($f_n < 2f_0$) corresponds to low values of x , which are generally associated with low energies, we do not require a relativistic correction. The simpler form of this nomogram is offset by the necessity of additional slide rule and arithmetical calculations.

The discussion so far has been limited to "original" or non-echoed hooks. However, the electromagnetic energy or signal may be reflected near the Earth back along the field line once (and so be observable near the conjugate point) or perhaps several times. Such echoed hooks can also be used for evaluation of electron parameters. The frequencies f_0 and f_n will be unchanged. From (10) we see that T^+ also will be unchanged. On the other hand the midpoint locus $\frac{1}{2}T^-$ for a non-echoed hook is the dispersion of a single trip from the equatorial plane to the Earth's surface. For a once-echoed hook the dispersion path is three times this so that T_n^- for such a hook is three times that of the original hook. Since a once-reflected hook is not easily recognized as such, calculation of scale frequency from T_n^- by Figure 3 would lead to a value nine times too large. Fortunately, however, such an ambiguity can usually be resolved. Carpenter (1962) measured f_n , t_n of over 250 whistlers. If these are converted to scale frequencies, about 75% lie in the range 0.5-2 Mc/s. The highest was about 4 Mc/s and for nose frequencies less than about 10 kc/s there was none above 2 Mc/s. Consequently, apparent values of $a > 2$ or 3 as obtained from T_n^- are evidence of echoed hooks. This ambiguity is completely removed if more than one echo is observed, as t_n can then be measured directly.

In general, the treatment given above can only be applied to complete emissions or hooks. Incomplete forms such as "falling tones" and "risers" only provide f_0 , and T_1 or T_2 . If the nose and scale frequencies are known from other data the missing parts could be supplied from the midpoint locus $\frac{1}{2}T^-$. This would be the case if identifiable echoes were observed.

The theory of this treatment is based on the assumption of a dipole magnetic field and a constant scale frequency along the field line within the region of generation of the observed frequencies. Some departures in the T^+ curve over that calculated from the theory have been noticed. As these occur at the high frequency end it is perhaps advisable to measure T^+ at the lower of the frequencies f_n and $2f_0$. These departures do not seem to occur in the T^- curve, indicating that any perturbations are symmetrical about the equatorial plane.

VI. SOME EXAMPLES

As an example of the method 14 hooks were scaled from spectrograms published by Gallet (1959) and by Helliwell and Carpenter (1961). These published spectrograms had the usual aspect ratio of 10 kc/s range being equivalent to 1 second interval, which is ideal for our purposes. The size, contrast, and definition of these spectrograms as published were not really suitable for accurate scaling but useful results were obtained, as shown in Table 1. The first five of these hooks were taken from Gallet and the remaining nine from Helliwell and Carpenter.

The sum time T^+ was measured at $2f_0$ for each hook and at f_n as well for six of these hooks. These times are shown in Table 1 as T_{20}^+ and T_n^+ respectively. For these six hooks both methods were used for energy and helical pitch calcu-

TABLE 1
ELECTRON DATA DEDUCED FROM HOOKS

No.	Measured					Deduced						
	f_0 (kc/s)	f_n (kc/s)	T_n^- (sec)	T_n^+ (sec)	T_{20}^+ (sec)	$\frac{1}{2}t_0$ (sec)	α^* (Mc/s)	λ	ψ_0	E (keV)	ψ_0^\dagger	E^\dagger (keV)
1	3.3	9.6	0.40	0.57	0.33	0.85	1.3	57°	64°	85	62°	78
2	3.3	5.7	0.22	0.56	0.70	1.3	1.8	60°	74°	47	70°	31
3	3.7	7.1	0.23	0.70	0.75	1.0	1.5	59°	58°	23	63°	29
4	2.7	5.3	0.35	0.78	0.80	1.5	1.7	60°	64°	26	66°	26
5	3.9	10.4	0.40	—	0.53	1.0	2.1	57°	56°	37	—	—
6	1.6	4.6	0.48	—	0.31	1.0	0.50	61°	68°	150	—	—
7	4.2	8.0	0.28	0.42	0.49	—	(2.8)	58°	50°	47	57°	60
8	2.7	7.5	0.28	—	0.43	0.65	0.53	58°	38°	55	—	—
9	1.6	6.5	0.61	—	0.36	0.95	0.59	59°	41°	70	—	—
10	2.0	6.5	0.44	—	0.42	0.85	0.56	59°	48°	68	—	—
11	2.3	6.5	0.44	—	0.38	1.0	0.82	59°	58°	83	—	—
12	2.1	6.5	0.35	—	0.38	0.70	0.40	59°	56°	80	—	—
13	3.2	7.1	0.28	0.56	0.48	0.95	1.1	59°	52°	51	56°	57
14	1.9	6.3	0.50	—	0.38	0.95	0.63	59°	55°	88	—	—

* Deduced from the hook. The value used for energy and pitch calculation may differ from this.

† Calculated by the alternative method (Fig. 5).

lation. The two sets of these values are shown in Table 1. There is reasonable agreement between them. What discrepancies there are could be explained by either scaling errors or the simplifying assumptions used in deriving the alternative (f_n) method.

The scale frequency a as calculated from Figure 3 for each hook is shown in Table 1. However, for the value adopted for energy and pitch calculation, use was made of the fact that hooks often occur in groups. For instance, the last seven hooks all occurred within 30 seconds or so of 0135 U.T. on October 6, 1959. Also hooks 2 and 3 both occurred at 0635 U.T. on February 15, 1958. It seems reasonable to assume that the scale frequency would not change in such a short time. Thus a weighted average value was adopted in such cases.

This sample is too small for statistical analysis. It seems that relatively few spectrograms of hooks have been actually published, though since 7 of the 14 considered here occurred in an interval of half a minute one would expect that enormous numbers would have been recorded during the I.G.Y. However, some interesting preliminary conclusions can be drawn from the few we have here.

Table 1 shows that the generation of these hooks was confined to a narrow range of field line latitudes. The last seven were observed at Seattle (geomagnetic latitude 54° N.) but barely or not at all at Stanford (44° N.), as shown in Helliwell and Carpenter (1961). This indicates an observing range for any one event (produced by propagation under the ionosphere) of some 10° of latitude. Thus we would predict from this that the occurrence rate of observations as a function of receiving station latitude should show a broad maximum in the vicinity of 59° . The observed (Helliwell and Carpenter 1961) occurrence rate of "chorus" for days of $K_p \geq 4$ shows such a maximum at approximately 58° . Although the average latitude of the field lines of generation can be deduced from such analyses of occurrence rate of observations, the method given here for the first time gives the latitude of *individual* emissions. The method also gives the time of generation of the centre (f_0) of the hooks. From Table 1 we see that this occurred about 1 second before observation.

If the electron bunches which produce these hooks were all injected into the field line near the equatorial plane and if there were no preferred direction of injection, one would expect the median of the equatorial pitch angle ψ_0 values of a large number of bunches to be 60° . This is approximately so for the 14 hooks in Table 1. The latitude angles of the mirror points (l_m) corresponding to these values of ψ_0 range from about 8° to 30° as seen from the top scale of Figure 4. The latitude angles of the points at which the frequency f_n was generated was found from η for the six hooks for which T_n^+ was scaled. These ranged from 7° to 14° . Thus most of the observed frequency range is generated within some 10 – 20° of the equatorial plane. It is important to note that, since f_n is the highest frequency at which measurements are made, the assumptions of constant scale frequency and dipole magnetic field need only apply within this region.

Probably the most important parameter is the electron energy. The energies shown in Table 1 are of the order of a few tens of kilo-electron-volts. Thus

typical values of β are around 0.3–0.5. Relativistic effects are very small at these velocities, so that the approximate correction formula (9) which was applied to the energy scale of Figure 4 should be sufficiently accurate.

VII. ACKNOWLEDGMENT

I am indebted to Professor G. R. A. Ellis of the Physics Department, University of Tasmania, for advice, criticism, and encouragement.

VIII. REFERENCES

- CARPENTER, D. L. (1962).—*J. Geophys. Res.* **67**: 135–45.
DOWDEN, R. L. (1962a).—*J. Geophys. Res.* **67**: 1745–50.
DOWDEN, R. L. (1962b).—*Nature* **195**: 1085–6.
DOWDEN, R. L. (1962c).—*Nature* **195**: 984–5.
EIDMAN, V. IA. (1958).—*J. Exp. Theor. Phys. (U.S.S.R.)* **34**: 131–8.
ELLIS, G. R. A. (1962).—*Aust. J. Phys.* **15**: 344–53.
GALLET, R. M. (1959).—*Proc. Inst. Radio Engrs.* **47**: 211–31.
HELLIWELL, R. A., and CARPENTER, D. L. (1961).—Whistlers—West I.G.Y.–I.G.C. Synoptic Program. S.E.L. Report March 20, Stanford University.
SMITH, R. L. (1960).—The use of nose whistlers in the study of the outer ionosphere. S.E.L. Report No. 6, Stanford University.
SMITH, R. L., and CARPENTER, D. L. (1961).—*J. Geophys. Res.* **66**: 2582–6.